0026-895X/02/6105-1070–1080$7.00
MOLECULAR PHARMACOLOGY
Copyright © 2002 The American Society for Pharmacology and Experimental Therapeutics
Mol Pharmacol 61:1070–1080, 2002

Vol. 61, No. 5
1486/976858
Printed in U.S.A.

Importance of the γ-Aminobutyric Acid$_B$ Receptor C-Termini for G-Protein Coupling

SYLVIA GRÜNEWALD, BETTINA J. SCHUPP, STEPHEN R. IKEDA,[1] ROHINI KUNER,[2] FRANK STEIGERWALD,[3] HANS-CHRISTIAN KORNAU,[4] and GEORG KÖHR

Axaron Bioscience AG, Heidelberg, Germany (S.G., R.K., H.-C.K.); Department of Molecular Neurobiology, Max-Planck-Institute for Medical Research, Heidelberg, Germany (B.J.S., G.K., F.S.); Laboratory of Molecular Physiology, Guthrie Research Institute, Sayre, Pennsylvania (S.R.I.)

Received November 9, 2001; accepted January 25, 2002

This article is available online at http://molpharm.aspetjournals.org

ABSTRACT

Functional γ-aminobutyric acid$_B$ (GABA$_B$) receptors assemble from two subunits, GABA$_{B(1)}$ and GABA$_{B(2)}$. This heteromerization, which involves a C-terminal coiled-coil interaction, ensures efficient surface trafficking and agonist-dependent G-protein activation. In the present study, we took a closer look at the implications of the intracellular C termini of GABA$_{B(1)}$ and GABA$_{B(2)}$ for G-protein coupling. We generated a series of C-terminal mutants of GABA$_{B(1)}$ and GABA$_{B(2)}$ and tested them for physical interaction, surface trafficking, coupling to adenylyl cyclase, and G-protein-gated inwardly rectifying potassium channels in human embryonic kidney (HEK) 293 cells as well as on endogenous calcium channels in sympathetic neurons of the superior cervical ganglion (SCG). We found that the C-terminal interaction contributes only partly to the heterodimeric assembly of the subunits, indicating the presence of an additional interaction site. The described endoplasmic reticulum retention signal within the C terminus of GABA$_{B(1)}$ functioned only in the context of specific amino acids, which constitute part of the GABA$_{B(1)}$ coiled-coil sequence. This finding may provide a link between the retention signal and its shielding by the coiled coil of GABA$_{B(2)}$. In HEK293 cells, we observed that the two well-known GABA$_B$ receptor antagonists [*S*-(R*,R*)]-[3-[[1-(3,4-dichlorophenyl)ethyl]amino]-2-hydroxypropyl](cyclohexylmethyl) phosphinic acid (CGP54626) and (+)-(2*S*)-5,5-dimethyl-2-morpholineacetic acid (SCH50911) CGP54626 and SCH50911 function as inverse agonists. The C termini of GABA$_{B(1)}$ and GABA$_{B(2)}$ strongly influenced agonist-independent G-protein coupling, although they were not necessary for agonist-dependent G-protein coupling. The C-terminal GABA$_B$ receptor mutants described here demonstrate that the active receptor conformation is stabilized by the coiled-coil interaction. Thus, the C-terminal conformation of the GABA$_B$ receptor may determine its constitutive activity, which could be a therapeutic target for inverse agonists.

GABA$_B$ receptors mediate metabotropic functions of the inhibitory neurotransmitter GABA via activation of G-proteins of the G$_{i/o}$ class. They inhibit adenylyl cyclase and modulate the activity of calcium and potassium channels, thereby controlling presynaptic neurotransmitter release and postsynaptic inhibitory potentials (Bowery, 1993). Impaired GABA$_B$ receptor function is associated with pathophysiological effects, including pain, epilepsy, spasticity, and cognitive deficits (Couve et al., 2000), which was recently highlighted in mice deficient for a GABA$_B$ receptor subunit (Prosser et al., 2001; Schuler et al., 2001).

Thus far, two GABA$_B$ receptor subunits, termed GABA$_{B(1)}$ and GABA$_{B(2)}$, have been cloned (Kaupmann et al., 1997, 1998; Jones et al., 1998; White et al., 1998; Kuner et al., 1999; Ng et al., 1999). Both subtypes exist in several splice forms, the most prominent being two N-terminal splice forms of GABA$_{B(1)}$, GABA$_{B(1a)}$, and GABA$_{B(1b)}$, whereby the first 147 residues in GABA$_{B(1a)}$ are replaced with 18 different residues in GABA$_{B(1b)}$ (Kaupmann et al., 1997). GABA$_B$ receptors belong to the C family of G-protein coupled receptors (GPCRs), which also comprises metabotropic glutamate, Ca^{2+}-sensing, and vomeronasal receptors. They all have an unusually large N-terminal, extracellular ligand binding domain that shows similarity to bacterial periplasmic amino

This work was supported by Bundesministerium für Bildung, Wissenschaft, Forschung und Technologie grant 0311633.

[1] Current address: National Institute on Alcohol Abuse and Alcoholism, National Institutes of Health, Bethesda, Maryland.

[2] Current address: Department of Molecular Pharmacology, University of Heidelberg, Heidelberg, Germany.

[3] Current address: Department of Physiology, University of Kiel, Kiel, Germany.

[4] Current address: Center for Molecular Neurobiology (ZMNH), University of Hamburg, Hamburg, Germany.

ABBREVIATIONS: GABA, γ-aminobutyric acid; GPCR, G-protein coupled receptor; HEK, human embryonic kidney; ER, endoplasmic reticulum; bp, base pair(s); PCR, polymerase chain reaction; cc, coiled-coil domain; NGS, normal goat serum; TBS, Tris-buffered saline; FSK, forskolin; GIRK, G-protein-activated inwardly rectifying potassium channel; SCG, superior cervical ganglion; SCH50911, (+)-(2*S*)-5,5-dimethyl-2-morpholineacetic acid; CGP54626, [*S*-(R*,R*)]-[3-[[1-(3,4-dichlorophenyl)ethyl]amino]-2-hydroxypropyl](cyclohexylmethyl) phosphinic acid; BAPTA, 1,2-bis(2-aminophenoxy)ethane-*N*,*N*,*N*′,*N*′-tetraacetic acid.

acid binding proteins (Couve et al., 2000). Although GPCRs were earlier generally believed to function as monomers, several GPCRs have been recently shown to exist as homo- as well as heterodimers that are functional and play important roles in signaling (Salahpour et al., 2000). C-family GPCRs are likely to function as dimers (Romano et al., 1996; Bai et al., 1999); also, A-family GPCRs (e.g., opioid receptor subtypes or dopamine and somatostatin receptors) have been shown to form homodimers and heterodimers, thereby creating new receptors with altered ligand binding and functional properties (Jordan and Devi, 1999; Rocheville et al., 2000a,b). $GABA_B$ receptors are unique in that complete functional activity depends on the formation of heteromers between $GABA_{B(1)}$ and $GABA_{B(2)}$. The monomeric receptor molecules alone are not able to reproduce the pharmacological properties of native $GABA_B$ receptors. Both splice forms $GABA_{B(1a)}$ and $GABA_{B(1b)}$ show lower affinity for agonists than native receptors but bind $GABA_B$ receptor antagonists with native affinity. $GABA_{B(2)}$ has not yet been shown to bind GABAergic ligands with appreciable affinity (Jones et al., 1998; Kaupmann et al., 1998). However, coexpression of $GABA_{B(2)}$ with $GABA_{B(1)}$ restores high-affinity agonist binding as well as regulation of intracellular effector systems (Jones et al., 1998; Kaupmann et al., 1998; White et al., 1998; Kuner et al., 1999; Ng et al., 1999). G-protein coupling seems to mainly involve intracellular loops of $GABA_{B(2)}$, but efficient G-protein coupling requires allosteric interactions of $GABA_{B(1)}$ with $GABA_{B(2)}$ (Galvez et al., 2001; Robbins et al., 2001).

$GABA_{B(1)}$ and $GABA_{B(2)}$ associate, at least partly, through a coiled-coil motif forming a parallel coiled-coil helix found in their respective C termini (Kammerer et al., 1999; Kuner et al., 1999). When expressed alone in human embryonic kidney (HEK) 293 cells or sympathetic neurons, $GABA_{B(1)}$ is retained in the endoplasmic reticulum (ER) (Couve et al., 1998) due to a C-terminal retention motif [RXR(R)] (Margeta-Mitrovic et al., 2000), which is located C-terminal of its coiled-coil region. Through this coiled-coil interaction, $GABA_{B(2)}$ masks the retention signal present in $GABA_{B(1)}$, thus enabling surface expression of functional $GABA_B$ receptors (Margeta-Mitrovic et al., 2000; Calver et al., 2001; Pagano et al., 2001).

Despite the discovery of structural elements for retention and interaction of $GABA_B$ receptor subunits, a detailed understanding of the functional role of $GABA_B$ receptor C termini is still lacking. The apparent interdependence of heterodimerization, surface trafficking and efficient G-protein coupling in vivo made it difficult to assess the exact molecular function of single domains or interactions within the $GABA_B$ receptor dimer. Thus, the aim of our study was to dissect these functions and to examine the role of defined C-terminal domains in heteromerization and signaling. We constructed several C-terminal mutant proteins of $GABA_{B(1)}$ and $GABA_{B(2)}$ and analyzed heterodimerization, cell surface expression, G-protein coupling, and constitutive activity in cotransfected HEK293 cells and in sympathetic neurons of the superior cervical ganglion (SCG).

Materials and Methods

Construction of Mutant Receptor Subunits. Cloning of full-length rat $GABA_{B(1a)}$ and $GABA_{B(2)}$ sequences was described in Kuner et al. (1999). The truncated and chimeric versions of $GABA_{B(1a)}$ were generated by PCR and subcloning of the PCR products into the *Pst*I (bp 2281) and *Sal*I sites of $GABA_{B(1)}$ in pBlueScript (Stratagene, La Jolla, CA). In $GABA_{B(1a)}\Delta CT$ and $GABA_{B(1a)}\Delta 924$–960, respectively, either the whole C terminus (amino acids R862 to K960) or amino acids R924 to K960 after the coiled-coil region were deleted. In the chimeric constructs $GABA_{B(1a)}$_2CT817–940 and $GABA_{B(1a)}$_2CT, either the C-terminal sequence of $GABA_{B(1a)}$ after the coiled-coil sequence (i.e., amino acids R924–K960) or the whole $GABA_{B(1a)}$ C terminus (amino acids R857–K960) was exchanged by overlap extension PCR for the equivalent sequences in $GABA_{B(2)}$ (i.e., amino acids D817–L940 or amino acids I744–L940, respectively). $GABA_{B(1a)}\Delta cc$ was constructed by ligating annealed complementary oligonucleotides with appropriate overhangs into the *Bcl*I (bp 2576) and *Nar*I (bp 2772) sites of $GABA_{B(1a)}$, yielding deletion of the coiled-coil encoding sequence (bp 2659–2763 encoding amino acids S887–L921). To allow surface detection of $GABA_{B(1a)}$ mutants, the sequence for the c-myc epitope was inserted behind the sequence of the predicted signal peptide by overlap extension PCR resulting in the encoded protein sequence ^{14}LGA**EQKLISEEDLN**GGA^{19} (c-myc epitope, including an additional N printed in bold).

In $GABA_{B(2)}\Delta 820$–940 and $GABA_{B(2)}\Delta CT$, the codons for amino acids E820–L940 and F761–L940 were deleted by PCR. For construction of $GABA_{B(2)}\Delta 748$–780 and $GABA_{B(2)}\Delta CT+cc$, two PCR fragments were generated that could be ligated through *Bam*HI, thereby replacing the codons covering the sequence between the end of transmembrane 7 and the coiled-coil sequence (amino acids T748–N780) by a single isoleucine codon (ATC). In $GABA_{B(2)}\Delta CT+cc$ the C-terminal sequence (amino acids E820–L940 after the $GABA_{B(2)}$ coiled-coil region) was deleted additionally. The coiled-coil deletion construct $GABA_{B(2)}\Delta cc$ and the chimeric construct $GABA_{B(2)}$_1CT922–960 were made by overlap extension PCR. In $GABA_{B(2)}\Delta cc$ amino acids S785–Q816 were deleted. For generating the chimeric construct $GABA_{B(2)}$_1CT922–960, the $GABA_{B(1)}$ C-terminal sequence (amino acids R922–K960 after the coiled-coil sequence) was amplified and exchanged for the corresponding C-terminal end of $GABA_{B(2)}$ (amino acids P819–L940) by overlap extension PCR. All constructs were cloned into a CMV expression vector (Schall et al., 1990). For constructing Flag-$GABA_{B(2)}$CT and Flag-$GABA_{B(2)}$CTΔcc, the C-terminal fragments (starting at I744) of $GABA_{B(2)}$ and $GABA_{B(2)}\Delta cc$ were amplified by PCR and cloned into a CMV expression vector (Schall et al., 1990) in frame behind the Flag-tag sequence, allowing the production of N-terminally Flag-tagged proteins. All constructs were verified by sequencing and are schematically shown in Fig. 1.

Antibodies. The $GABA_{B(1)}$-specific polyclonal antiserum was bought from BD PharMingen (San Diego, CA) and is directed against the last 20 amino acids (941–960) in $GABA_{B(1a)}$. $GABA_{B(2)}$ -specific antisera were raised against two synthetic peptides, one derived from amino acids 203 to 222 in the N-terminal extracellular domain (DVQRFSEVRNDLTGVLYGED-amid) and the second corresponding to amino acids 831 to 850 in the C terminus of $GABA_{B(2)}$ (QELNDILSLGNFTESTDGGK-amid). Peptide synthesis, antibody generation and purification were done by ARK Scientific GmbH Biosystems (Darmstadt, Germany). The titers of the crude sera (as defined in an enzyme-linked immunosorbent assay test as the reciprocal of the serum dilution resulting in an OD_{492} of 0.2 when using 1 μg of free antigen on the solid phase per well) were 66,000 for the serum recognizing the N-terminally located peptide sequence and 300,000 for the serum recognizing the C-terminally located peptide sequence, respectively. For detection of the myc epitope tag, a rabbit polyclonal anti-Myc tag IgG antibody (Upstate Biotechnology, Lake Placid, NY) was used. Peroxidase- and tetramethylrhodamine B isothiocyanate-conjugated secondary antibodies were bought from Jackson ImmunoResearch Laboratories (West Grove, PA).

Cell Culture and Transfection. HEK293 cells were maintained in modified Eagle's medium (MEM; Invitrogen, Carlsbad, CA) supplemented with 10% fetal bovine serum and PenStrep at 37°C with 5% CO_2. Cells were transfected at 70% confluence with 25 μg of total

DNA for a 15-cm plate or 2.5 μg of DNA for a 24-well coverslip by calcium phosphate precipitation. Cells were incubated for 2 days before testing expression of recombinant proteins or performing functional assays.

Receptor Binding Assays. Transfected cells were harvested, washed once in phosphate-buffered saline (PBS) or Krebs-Tris buffer (20 mM Tris-HCl, pH 7.4, 118 mM NaCl, 1.2 mM KH_2PO_4, 1.2 mM $MgSO_4$, 4.7 mM KCl, 1.8 mM $CaCl_2$, and 5.6 mM glucose) and incubated in PBS or Krebs-Tris-buffer with 10 nM [^{3}H]CGP54626A (Tocris Cookson Ltd., Bristol, UK) for 1 h at room temperature (RT). The incubation was terminated by addition of 3 ml of cold washing buffer (50 mM Tris-HCl, 150 mM NaCl, pH 7.4) and rapid vacuum filtration over Whatman GF/C filters prewashed with 2 ml of washing buffer. The filters were washed twice with 3 ml of cold washing buffer and counted for tritium using a Tri-Carb scintillation counter (Canberra EuriSys GmbH, Rüsselsheim, Germany). Nonspecific binding was determined either with 10 μM CGP54626 or with 2 mM SCH50911 (Tocris Cookson).

Coimmunoprecipitation and Immunoblot Analysis. Transfected HEK293 cells were collected 48 h after transfection and solubilized over night by gentle rotation at 4°C with 2% Triton X-100 in PBS containing 400 mM NaCl and 10% glycerol as well as the protease inhibitors phenylmethylsulfonyl fluoride (1 mM), leupeptin (10 μg/ml), aprotinin (10 μg/ml), pepstatin A (5 μg/ml), and chymostatin (5 μg/ml). After ultracentrifugation at 100,000*g* for 1 h at 4°C, the supernatant was diluted 2-fold in PBS and rotated with 1/100 volume (i.e., 8 μl) of preimmuneserum for 1 h at 4°C. For clearance of unspecific immunocomplexes 20 μl of protein A-Sepharose (Sigma, St. Louis, MO) were added and incubation continued for 1 h. Then, the supernatant of the protein A-Sepharose beads was rotated with 1/100 volume (i.e., 8 μl) of the $GABA_{B(2)}$ -C terminus–specific antipeptide antiserum for 1 h at 4°C. Immunocomplexes were precipitated for 1 to 2 h at 4°C again with 20 μl of protein A-Sepharose. The captured immunocomplexes of both the incubation with preimmuneserum and antiserum were washed 4 times with PBS containing 1% Triton X-100 and once with PBS containing 0.5% Triton X-100 before eluting into sample buffer (50 mM Tris-HCl, pH 8.5, 200 mM dithiothreitol, 6% SDS, 10% glycerol, 7 M urea, 0.01% bromphenol blue) at 42°C for 10 min. Samples were resolved through 6% SDS-polyacrylamide gel electrophoresis and electrophoretically transferred to nitrocellulose membranes. After blocking with 5% nonfat dry milk powder in PBS containing 0.2% Tween 20, the nitrocellulose membranes were probed with the $GABA_{B(1)}$-specific antiserum, diluted 1:2000 in blocking solution, for 1 h at room temperature, followed by three 5-min washes in PBS containing 0.2% Tween 20 and incubation with horseradish peroxidase-labeled anti-guinea pig antibodies. Bound antibody was visualized by enhanced chemiluminescence (enhanced chemiluminescence; Amersham Biosciences, Freiburg, Germany).

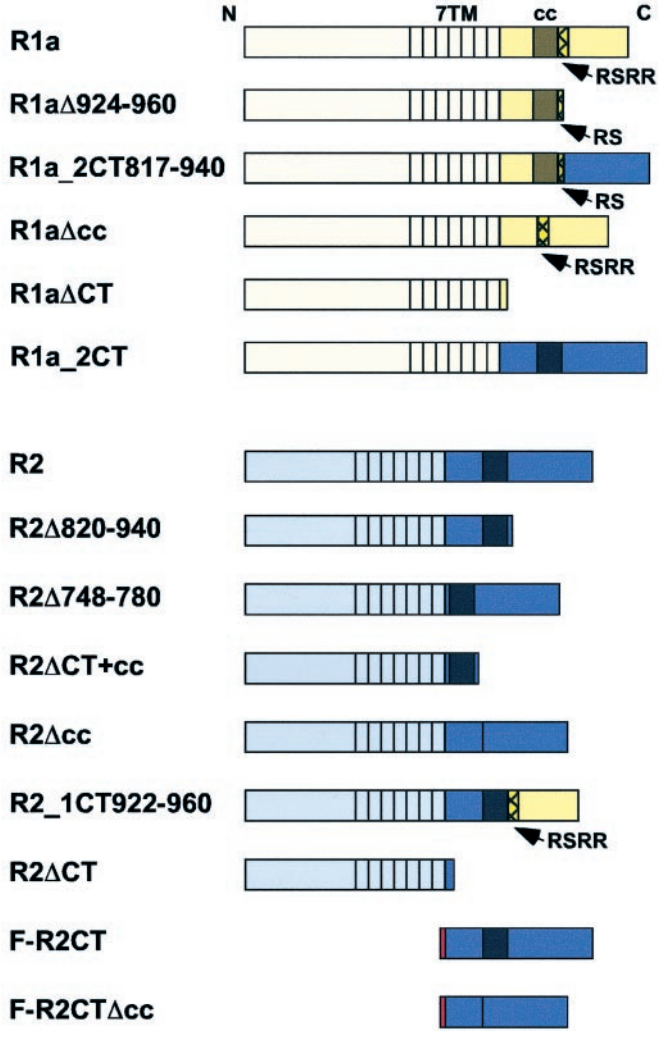

Fig. 1. Schematic outline of $GABA_B$ receptor subunit constructs. N, large extracellular N-terminal domain; 7TM, domain including the seven transmembrane helices; cc, predicted coiled-coil region in both the C terminus of $GABA_{B(1)}$ (R1) and $GABA_{B(2)}$ (R2); RSRR, endoplasmic reticulum retention signal; F, Flag-tag (red); C, C terminus, which is depicted as enlarged relative to other domains.

Immunocytochemistry. Cells were seeded and grown on sterile glass coverslips coated with either fibronectin (10 μg/ml) or poly-D-lysine (5 μg/ml) and transfected with various receptor mutant constructs 2 days before immunocytochemical analysis. For analyzing receptor expression, cells were washed twice with PBS, fixed on ice for 10 min in 2% paraformaldehyde/0.2% glutaraldehyde, incubated twice for 5 min each in 50 mM glycine in PBS, and washed with PBS. For permeabilization, cells were incubated with 0.2% Triton X-100 in PBS for 10 min on ice and blocked for 30 min at RT with 4% normal goat serum (NGS) and 0.2% Triton X-100 in cold PBS. Primary antibody incubations (anti-Myc IgG, 1:200; anti-$GABA_{B(2)}$ antibodies, 1:100 or 1:200) were in 2% NGS and 0.1% Triton X-100 in cold Tris-buffered saline (TBS; 10 mM Tris-HCl, 100 mM NaCl, pH 7.6) for 2 to 3 h at RT. After three 10 min washes with 1% NGS in TBS at RT, the cells were incubated with donkey–anti-rabbit tetramethylrhodamine B isothiocyanate-conjugated antibody (1:400) in 1.5% NGS in TBS in the dark for 30 min at RT. After several washing steps, cover slips were mounted and analyzed using a confocal microscope (Leica Mikrosysteme Vertrieb GmbH, Bensheim, Germany).

For localization of receptor proteins at the cell surface, intact cells were washed with PBS and incubated for 1 h at 4°C with the primary antibody in PBS containing 2% NGS for blocking. Then, cells were fixed and incubated with the secondary antibody as described above.

Cellular cAMP Accumulation Assay. Two days before the assay, HEK293 cells plated onto 15-cm plates were cotransfected with various combinations of $GABA_B$ receptor subtype mutants. On the day of the assay, the medium was replaced by MEM medium supplemented with 1 mM 3-isobutyl-1-methylxanthine (Sigma) and the cells were incubated for 15 min at 37°C and 5% CO_2. The cells were harvested and resuspended to 2.5×10^6 cells/ml in Krebs-Tris buffer supplemented with 1 mM 3-isobutyl-1-methylxanthine. These cells (200 μl; 0.5×10^6 cells) were added to tubes containing either no drugs (basal activity), 2 μM forskolin (FSK), or 2 μM FSK plus GABA-ergic agonists [e.g., 100 μM (*R*)-baclofen (Tocris Cookson)] or antagonists [e.g., 10 μM CGP54626 (Tocris Cookson)] as indicated in the figure legend. After 20 min at 37°C, the tubes were placed on ice and lysed in 167 mM HCl. The lysate was incubated on ice for at least 1 h and, after neutralization with NaOH, was centrifuged at 15,000*g* to remove cell debris. The cellular production of cAMP was measured in the supernatant using the commercially available cAMP ^{3}H assay

system from Amersham Biosciences. Experiments were performed at least twice in duplicate. The significance of differences was evaluated using unpaired, two-tailed Student's *t*-tests.

Coupling to GIRKs. Coexpression of GIRK1 and GIRK2 with $GABA_{B(1a)}$ and $GABA_{B(2)}$ wild-type or mutant constructs was as described by Kuner et al. (1999). Transfected cells on coverslips were transferred to the stage of an inverted microscope and were continuously perfused with a solution containing 115 mM NaCl, 25 mM KCl, 1.8 mM $CaCl_2$, 1 mM $MgCl_2$, 5 mM HEPES, and 10 mM glucose, pH 7.25, adjusted with NaOH. The whole-cell configuration of the patch-clamp technique was applied at RT with pipette solutions containing 115 mM K-gluconate, 20 mM KCl, 10 mM HEPES, 5 mM EGTA, 4 mM MgATP, and 0.3 mM NaGTP, pH 7.25, adjusted with KOH. GABA (100 μM) or (*R*)-baclofen (50 μM) was dissolved in the extracellular solution and was applied steadily to single cells by a double-barreled application pipette. The inward rectifier currents were activated by voltage ramp generation. For analysis, GIRK-currents in the absence and presence of agonist were compared at −135 mV. Values are expressed as mean ± S.E.M. and *p*-values represent the result of independent two-tailed *t*-tests.

Ca^{2+}-Channel Current Recordings. Superior cervical ganglion (SCG) neurons were isolated and injected with cDNA as described previously (Ikeda, 1996; Ikeda, 1997). Briefly, SCG neurons were enzymatically dissociated from adult rats and then plated onto polystyrene culture dishes (35 mm), coated with poly-L-lysine, and maintained in a humidified atmosphere of 95% air/5% CO_2 at 37°C. $GABA_B$ receptor subunits were expressed by intranuclear microinjection (0.1 μg/μl per cDNA construct). Electrophysiological recordings were made within 24 h after injection of vectors. Injected neurons were identified by fluorescence from coexpressed jellyfish green fluorescent protein (enhanced green fluorescent protein; BD Biosciences Clontech, Palo Alto, CA).

Ca^{2+} channel currents were recorded at RT using the whole-cell variant of the patch-clamp technique as described previously (Ikeda, 1996). To isolate Ca^{2+} currents, patch electrodes were filled with a solution containing 125 mM *N*-methyl-D-glucamine methanesulfonate, 20 mM tetraethylammonium Cl, 15 mM CsCl, 10 mM BAPTA, 1 mM $CaCl_2$, 10 mM HEPES, 4 mM MgATP, 0.1 mM GTP, 5 mM di-Tris phosphocreatine, pH 7.2 (304 mOsm/kg H_2O). The external recording solution contained 145 mM tetraethylammonium methanesulfonate, 10 mM HEPES, 10 mM $CaCl_2$, 15 mM glucose, 0.0003 mM tetrodotoxin, pH 7.4 (328 mOsm/kg H_2O). Agonists were applied to single neurons via a gravity-fed fused silica capillary tube connected to an array of seven polyethylene tubes. The outlet of the perfusion system was located within 100 μm of the cell. Drug application was started by switching the control external solution to a drug-containing solution. Calcium currents were evoked by a depolarizing pulse to +10 mV from a holding potential of −80 mV. Current amplitude was measured 10 ms after the onset of the test pulse. The inhibition of Ca^{2+} channel currents was tested with noradrenaline and was comparable in uninjected and injected neurons (not shown). Values are expressed as mean ± S.E.M.; *p*-values were determined by analysis of variance followed by Student-Newman-Keuls post hoc test.

Results

Interactions between Coiled-Coil Deletion Mutants of $GABA_{B(1)}$ and $GABA_{B(2)}$

To assess the role of C-terminal domains of $GABAB_{(1a)}$ and $GABA_{B(2)}$ for interaction, trafficking, and function of the $GABA_B$ receptor, we generated a series of deletion mutants (Fig. 1). These include specific deletions of the 35 and 32 amino acids in $GABA_{B(1a)}$ and $GABA_{B(2)}$, respectively, which have been shown to mediate a coiled-coil interaction (Kuner et al., 1999; $GABA_{B(1a)}\Delta$cc and $GABA_{B(2)}\Delta$cc). To test the importance of the C-terminal coiled-coil interaction for the integrity of the $GABA_B$ receptor, we performed coimmunoprecipitations using full-length proteins. Combinations of wild-type and coiled-coil deletion constructs were cotransfected into HEK293 cells and $GABA_{B(2)}$ or $GABA_{B(2)}\Delta$cc was immunoprecipitated from Triton X-100 extracts with preimmuneserum (PIS) followed by an antiserum (AS) directed against the C terminus of $GABA_{B(2)}$. The immunoprecipitated protein was blotted and analyzed for coprecipitation of $GABA_{B(1a)}$ or $GABA_{B(1a)}\Delta$cc (Fig. 2A). $GABA_{B(2)}$ not only precipitated $GABA_{B(1a)}$ but also $GABA_{B(1a)}\Delta$cc. Furthermore, $GABA_{B(2)}\Delta$cc was also able to precipitate $GABA_{B(1a)}$ and $GABA_{B(1a)}\Delta$cc. In all cases, the appropriate preimmuneserum did not lead to precipitation of $GABA_{B(1a)}$ or $GABA_{B(1a)}\Delta$cc (Fig. 2A, PIS). Coimmunoprecipitation of $GABA_B$ receptor wild-type proteins was most efficient (Fig. 2A, AS). We also analyzed the interaction of the soluble C-terminal fragments of $GABA_{B(1)}$ and $GABA_{B(2)}$. In both yeast two-hybrid assays and glutathione *S*-transferase pull-down assays, deletion of the coiled-coil region in one of the fragments abolished the interaction (not shown). These data suggest that interaction domains outside the cytoplasmic C termini of $GABA_{B(1)}$ and $GABA_{B(2)}$, in addition to the coiled-coil domains within the cytoplasmic C termini, mediate assembly of $GABA_B$ receptor heteromers.

C-Terminal Determinants of $GABA_B$ Receptor Surface Expression

In the absence of $GABA_{B(2)}$, $GABA_{B(1a)}$ is retained in the ER (Couve et al., 1998). However, $GABA_{B(1a)}$ efficiently reaches the cell surface after coexpression of $GABA_{B(2)}$ (White et al., 1998; Margeta-Mitrovic et al., 2000).

We tested the relevance of C-terminal stretches of the two subunits for $GABA_B$ receptor trafficking. The plasma membrane targeting of $GABA_{B(1a)}$ and $GABA_{B(2)}$ mutants expressed in HEK293 cells was examined by immunocytochemistry using antisera directed against extracellular N-terminal epitopes. This enabled staining of receptors targeted to the cell membrane in nonpermeabilized cells [surface staining (ST)] compared with those present at the membrane and in the cell interior in detergent permeabilized cells (P) (Fig. 2, B-D).

All $GABA_{B(1a)}$ deletion and chimeric mutants were expressed to a similar extent and, except for the full-length $GABA_{B(1a)}$ protein, were all found to be located at the plasma membrane (Fig. 2B). All $GABA_{B(2)}$ mutants were expressed at the cell surface, but in $GABA_{B(2)}\Delta$CT transfections, comparably fewer cells were found to be surface stained and staining was less intense (Fig. 2C). The total expression of $GABA_{B(2)}\Delta$748–780 and $GABA_{B(2)}\Delta$CT+cc seemed to be lower than that of the remaining $GABA_{B(2)}$ mutants (Western blot data not shown). In cotransfected HEK293 cells, all $GABA_{B(2)}$ mutants which still possessed the coiled-coil region (i.e., $GABA_{B(2)}\Delta$820–940, $GABA_{B(2)}$–1CT922–960, $GABA_{B(2)}\Delta$748–780, and $GABA_{B(2)}\Delta$CT+cc) were able to traffick $GABA_{B(1a)}$ to the cell surface; $GABA_{B(2)}\Delta$820–940 was the most efficient (Fig. 2D and Table 1). Interestingly, $GABA_{B(2)}$ subunits lacking the coiled-coil domain were able to traffick $GABA_{B(1a)}$ to the cell surface as well, yet to a smaller extent. Even in $GABA_{B(1a)}$ + $GABA_{B(2)}\Delta$CT cotransfections, a few cells per dish showed surface staining (Fig. 2D). The observed plasma membrane targeting of $GABA_{B(1a)}$ by $GABA_{B(2)}\Delta$cc and $GABA_{B(2)}\Delta$CT may result from both

additional interaction sites between $GABA_{B(1)}$ and $GABA_{B(2)}$ located outside their C termini and the strong overexpression of the two membrane proteins in transiently transfected cells. Furthermore, the C terminus of $GABA_{B(2)}$ expressed as a cytoplasmic protein (Flag-$GABA_{B(2)}$CT) prevented retention of $GABA_{B(1a)}$, whereas the C terminus of $GABA_{B(2)}$ lacking the coiled-coil sequence (Flag-$GABA_{B(2)}$CTΔcc) did not (Fig. 2D). These data substantiate recent reports on a role for the coiled-coil interaction in masking the retention signal in $GABA_{B(1)}$ (Calver et al., 2001; Margeta-Mitrovic et al., 2000; Pagano et al., 2001).

A new aspect of the molecular determinants of $GABA_{B(1)}$ retention emerged when studying surface trafficking of two of our mutants. $GABA_{B(1a)}$Δcc and $GABA_{B(2)}$_1CT922–960 have an intact ER retention signal RSRR but are still very efficiently transported to the cell surface (Fig. 2, B and C). In the construct $GABA_{B(1a)}$Δcc, the 35 codons encoding the putative coiled-coil sequence, directly upstream of the sequence for the retention signal, have been deleted. In $GABA_{B(2)}$_1CT922–960, the C terminus of $GABA_{B(1a)}$ distal of the coiled-coil region but including the retention signal was fused to the end of the coiled-coil region in $GABA_{B(2)}$ (Fig. 1). These data suggest that sequences upstream of the RSRR signal are required for intracellular retention of the receptor.

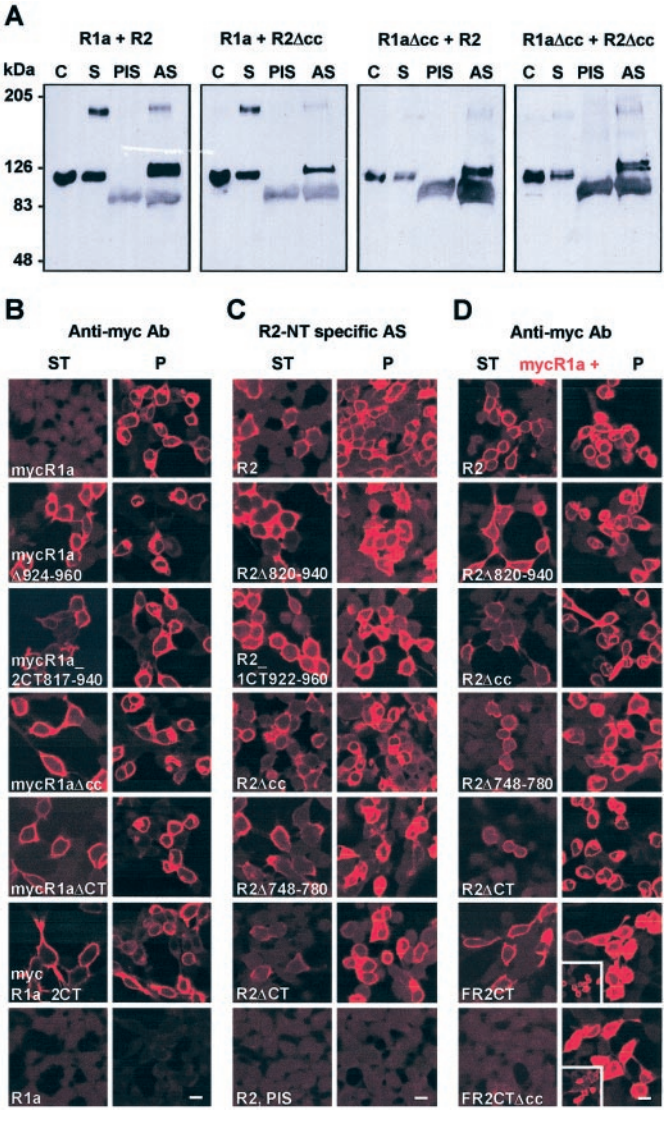

Fig. 2. A, coimmunoprecipitation of $GABA_{B(1a)}$ (R1a) and $GABA_{B(2)}$ (R2) coiled-coil deletion mutants. Extracts from HEK293 cells cotransfected with the indicated constructs were immunoprecipitated with the $GABA_{B(2)}$ -specific antiserum recognizing the C terminus (AS) or the appropriate preimmuneserum (PIS). The immunoprecipitates were immunoblotted for $GABA_{B(1)}$ (C, SDS-cell extract; S, solubilized protein fraction used for immunoprecipitation). B to D, surface trafficking of mutated $GABA_B$ receptor subunits. HEK293 cells grown on glass coverslips were transfected with constructs encoding either wild-type or mutant forms of $GABA_{B(1a)}$ (B), $GABA_{B(2)}$ (C), or both (D). All $GABA_{B(1a)}$ constructs were tagged N-terminally with a c-myc epitope recognized by a polyclonal anti-myc antibody (mycR1a). Two days after transfection, the cells were examined by immunofluorescence using the anti-myc antibody or a $GABA_{B(2)}$-specific polyclonal antiserum directed against the N terminus without [surface staining (ST)] or with permeabilization (P). The bottom panels in B and C are controls (R1a, nontagged wild-type $GABA_{B(1a)}$; PIS, preimmuneserum). D, insets, immunofluorescence of the soluble Flag-tagged $GABA_{B(2)}$ constructs using the $GABA_{B(2)}$C terminus-specific antiserum. Immunofluorescence analysis was done on at least three independent transfections for all combinations shown with consistent results. Scale bar, 10 μm.

The $GABA_B$ Receptor C Termini Are Not Necessary for Agonist-Mediated Effector Coupling

Coupling to Adenylyl Cyclase. We next examined whether C-terminal domains in $GABA_{B(1)}$ and $GABA_{B(2)}$ play a role in effector coupling. HEK293 cells were transiently cotransfected with combinations of wild-type or deletion mutants of the $GABA_B$ receptor subunits, and the effect of receptor activation on FSK-induced intracellular cAMP accumulation was measured. In all experiments, protein levels of $GABA_{B(1a)}$ and $GABA_{B(2)}$ mutants were controlled by Western blotting (data not shown) and [^{3}H]CGP54626 binding. Binding-active protein levels of $GABA_{B(1a)}$ and derived mutants in cotransfected HEK293 cells were comparable with 0.5 to 1.5 × 10^6 receptors/cell.

In HEK293 cells producing wild-type $GABA_{B(1a)}$ + $GABA_{B(2)}$ receptors, saturating concentrations of the GABAergic agonists GABA (500 μM, Fig. 3A) and (*R*)-baclofen (500 μM, Fig. 3A and 100 μM, Fig. 4A) inhibited 2 μM FSK-stimulated cAMP production by 40 to 60%. This inhibition could be antagonized by the $GABA_{B(1)}$-specific antagonists SCH50911 and CGP54626 (Figs. 3A and 4A). Coiled-coil deletion mutants (Fig. 3A) and $GABA_{B(2)}$ mutants, examined in combination with either $GABA_{B(1a)}$ (Fig. 4A) or $GABA_{B(1a)}$ΔCT (Fig. 4B), which ensures its unrestricted surface expression (Fig. 2B), did not show a significant difference in cAMP coupling compared with the wild-type combination. One exception was $GABA_{B(2)}$ΔCT, which in combination with $GABA_{B(1a)}$ showed reduced inhibition of FSK-stimulated cAMP accumulation compared with either the wild-type $GABA_B$ receptor ($p < 0.05$) or the double deletion mutant $GABA_{B(1a)}$ΔCT + $GABA_{B(2)}$ΔCT ($p < 0.05$).

Coupling to K^+ Currents. To investigate $GABA_B$ receptor regulation of potassium currents, we reconstituted $GABA_B$ receptor heterodimers of wild-type and/or mutated $GABA_B$ receptor subunits with GIRK1 and GIRK2 in HEK293 cells. Baclofen (or GABA) application to HEK293 cells led to robust increases in potassium conductance through GIRK-activation in the presence of all tested combinations by 57 to 150% (Figs. 3B and 4), except for $GABA_{B(1a)}$ + $GABA_{B(2)}$Δcc (Fig. 3B), $GABA_{B(1a)}$ + $GABA_{B(2)}$ΔCT, and $GABA_{B(1a)}$ΔCT + $GABA_{B(2)}$ΔCT (Fig. 4 and Table 1). The smaller ($p < 0.01$) conductance increases compared with

wild-type may have resulted from reduced surface expression, as shown for $GABA_{B(2)}\Delta CT$ when expressed alone (Fig. 2C) or for $GABA_{B(1a)}$ in the combinations mentioned above (Fig. 2D). However, 6 of 25 cells transfected with $GABA_{B(1a)}$ + $GABA_{B(2)}\Delta CT$ and two of nine cells transfected with $GABA_{B(1a)}\Delta CT$ + $GABA_{B(2)}\Delta CT$ showed GIRK-current activation comparable with other deletion mutants [68.1 ± 20% (n = 6) and 49.4% (n = 2)]. This is consistent with the observation that only a small fraction of cells transfected with $GABA_{B(1a)}$ + $GABA_{B(2)}\Delta CT$ expresses $GABA_{B(1a)}$ on the cell surface. Thus, GIRK-activation is also possible in the absence of $GABA_B$ receptor C termini.

Coupling to Ca^{2+} Currents. To investigate GABA-ergic inhibition of neuronal calcium channel currents, we microinjected plasmids encoding wild-type and/or mutated $GABA_B$ receptor subunits into the nucleus of SCG neurons. In SCG neurons that endogenously express $GABA_{B(1a)}$ and calcium channels, a significant ($p < 0.05$) baclofen-mediated inhibition of calcium conductance was obtained only when $GABA_{B(2)}$ was injected (Fig. 3C; see also Filippov et al., 2000). An increased ($p < 0.05$) calcium current inhibition was observed when coinjecting $GABA_{B(1a)}$ + $GABA_{B(2)}$, $GABA_{B(1a)}\Delta cc$ + $GABA_{B(2)}$, and $GABA_{B(1a)}\Delta cc$ + $GABA_{B(2)}\Delta cc$ (Fig. 3C). Similar to the results in GIRK channel coupling in HEK293 cells, injection of $GABA_{B(1a)}$ + $GABA_{B(2)}\Delta cc$ (Fig. 3C) or $GABA_{B(1a)}$ + $GABA_{B(2)}\Delta CT$ (Fig. 4A) resulted in a smaller ($p < 0.05$) calcium current inhibition in SCG neurons (see *Discussion*). Thus, the cytoplasmic C-terminal domains of $GABA_{B(1)}$ and $GABA_{B(2)}$ do not seem to be involved in the agonist-activated G-protein coupling of $GABA_B$ receptors in either HEK293 cells or neurons.

$GABA_B$ Receptor Antagonists Increase cAMP Levels in Cotransfected HEK293 Cells

When performing cAMP assays, we observed that antagonists not only block GABA-ergic agonist-mediated cAMP decrease but also increase cAMP levels above those induced with FSK alone (Fig. 4). We therefore looked at the direct effect of the antagonists SCH50911 and CGP54626 on FSK-induced cAMP levels and found that both antagonists increased cAMP accumulation up to 100% (Fig. 5A). The EC_{50} values of 1.67 ± 0.51 μM for SCH50911 (n = 4) and 6.7 ± 1.1 nM (n = 3) for CGP54626 were greater than their dissociation constants [IC_{50} = 0.43 ± 0.04 μM for SCH50911 (Kaupmann et al., 1998), K_D = 1.3 ± 0.1 nM for CGP54626; data not shown]. Treating transfected HEK293 cells with 100 ng/ml pertussis toxin, which ADP-ribosylates and inactivates G_i and G_o, for 16 h before assay eliminated both the G_i-mediated inhibition of FSK-stimulated cAMP accumulation by GABA or (*R*)-baclofen (not shown) as well as the increase of FSK-stimulated cAMP accumulation by SCH50911 or CGP54626 (Fig. 5C). These antagonists also increased basal cAMP levels up to 60% (not shown). However, basal cAMP levels are near the detection limit of our assay, so dose-response curves were not measured.

Interestingly, both antagonists had no effect on FSK-in-

TABLE 1

Coupling of recombinant $GABA_B$ receptors to effectors and surface localizaton of myc-tagged $GABA_{B(1a)}$ mutants

HEK293 cells were cotransfected with the constructs indicated and surface immunostaining as well as coupling to adenylyl cyclase and GIRKs was measured as outlined under *Materials and Methods*. Inhibition of Ca^{2+} currents was measured in SCG neurons.

Subunit Combinations	Agonist-Induced Decrease of cAMP Levels	Agonist-Induced Activation of GIRKs	Agonist-Induced Inhibition of Ca^{2+} Channels	Antagonist-Induced Increase of cAMP Levels	Surface Immuno-Staining of $GABA_{B(1a)}$ Constructs
Wild-Type					
R1a + R2	++	++	++	++	Yes
Coiled-Coil Deletion Mutants					
R1a + R2Δcc	++	+	+	–	Red.
R1aΔcc + R2	++	++	++	+	Yes
R1aΔcc + R2Δcc	++	++	++	–	Yes
R1a + R2 Mutants					
R1a + R2Δ820–940	++	++	N.D.	++	Yes
R1a + R2Δ748–780	++	++	N.D.	++	Red.
R1a + R2ΔCT+cc	++	N.D.	N.D.	++	Red.
R1a + R2ΔCT	+	+	+	–	Red.
R1a + R2_1CT922–960	++	N.D.	N.D.	++	Yes
R1a + FR-2CT	–	N.D.	N.D.	–	Yes
R1a + FR-2CTΔcc	N.D.	N.D.	N.D.	N.D.	No
R1aΔCT + R2 Mutants					
R1aΔCT + R2	++	++	N.D.	+	Yes
R1aΔCT + R2Δ820–940	++	++	N.D.	+	Yes
R1aΔCT + R2Δ748–780	++	++	N.D.	–	Yes
R1aΔCT + R2ΔCT+cc	++	++	N.D.	–	Yes
R1aΔCT + R2Δcc	++	++	N.D.	–	Yes
R1aΔCT + R2ΔCT	++	+	N.D.	–	Yes
Further R1a and R2 Mutants					
R1aΔ924–960 + R2	++	N.D.	N.D.	++	Yes
R1aΔ924–960 + R2Δ748–780	++	N.D.	N.D.	++	Yes
R1aΔ924–960 + R2Δ820–940	++	N.D.	N.D.	++	Yes
R1a_2CT817–940 + R2	++	N.D.	N.D.	++	Yes
R1a_2CT817–940 + R2Δ820–940	++	N.D.	N.D.	++	Yes
R1a_2CT817–940 + R2_1CT922–960	++	N.D.	N.D.	++	Yes
R1a_2CT + R1a	–	N.D.	N.D.	–	Yes
R1a_2CT + R2ΔCT	++	++	N.D.	N.D.	Yes

++, no significant difference in effector coupling compared with wild-type $GABA_B$ receptors ($p > 0.05$).
+, significantly reduced coupling compared with wild type ($p < 0.05$).
–, FSK-induced cAMP level did not change in the presence of GABA-ergic ligands ($p > 0.05$).
Red., reduced surface staining compared with wild-type $GABA_B$ receptors; N.D., not determined.

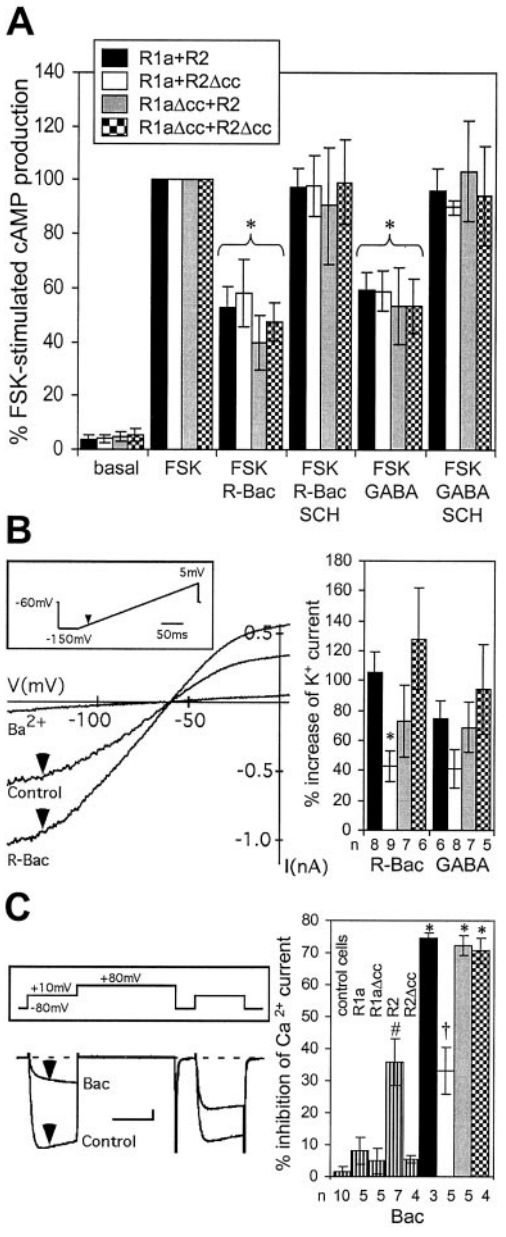

Fig. 3. Coupling of $GABA_{B(1a)}$ and $GABA_{B(2)}$ coiled-coil deletion mutants to effector proteins. A, inhibition of adenylyl cyclase. HEK293 cells were cotransfected with the indicated constructs. Two days later the influence of 500 μM (*R*)-baclofen (*R*-Bac) or 500 μM GABA in the absence or presence of 2 mM SCH50911 (SCH) on cAMP levels induced by 2 μM FSK was measured as outlined under *Materials and Methods*. "Basal" indicates cAMP levels in the absence of any drug. FSK-induced cAMP levels were set to 100%. The bar graph shows the percentage of FSK-stimulated cAMP production under the indicated condition. Error bars indicate the S.D. resulting from at least three independent transfections. The asterisks (*$p < 0.01$) refer to the effect of *R*-Bac and GABA on FSK-induced cAMP levels. B, GIRK-currents. Representative whole-cell recordings are shown from transfected HEK293 cells expressing functional $GABA_{B(1a)}$ + $GABA_{B(2)}$ receptors and GIRK1 and GIRK2. GIRK-currents (Control), which are barium sensitive (Ba^{2+}), were activated by 50 μM *R*-Bac. The voltage ramp used for current activation is shown above the current-voltage relationship. The currents represent averages of five current traces. Arrowhead, membrane potential (−135 mV) at which the currents were analyzed. The bar graph compares the GIRK-current increases in the presence of different $GABA_B$ deletion mutants (see A) caused by 50 μM *R*-Bac or 100 μM GABA. Error bars indicate mean ± S.E.M. (n, number of cells recorded). *, $p < 0.01$ compared with wild-type $GABA_B$ receptors. C, calcium channel currents. Representative whole-cell recordings are shown from rat SCG neurons heterologously expressing $GABA_{B(1a)}$ + $GABA_{B(2)}$ in the absence (Control) or presence of 300 μM baclofen (Bac). Currents were evoked with the double pulse voltage protocol illustrated. Current amplitude was determined 10 ms after the onset of the first test pulse (arrowhead). Horizontal and vertical calibration bars represent 20 ms and 0.5 nA, respectively. The bar graph indicates inhibition of calcium current in the presence of 300 μM Bac after expression of the indicated $GABA_B$ combination (see inset in A) in SCG neurons. Error bars indicate mean ± S.E.M. (*n*, number of neurons recorded). *, $p < 0.05$ for double-injected neurons compared with $GABA_{B(2)}$-injected neurons; †, $p < 0.05$ compared with neurons injected with wild-type receptors; #, $p < 0.05$ for $GABA_{B(2)}$-injected neurons compared with control cells.

duced cAMP levels in HEK293 cells cotransfected with $GABA_{B(1a)}$ and $GABA_{B(2)}\Delta cc$ (Fig. 5, A and D). In HEK293 cells expressing $GABA_{B(1a)}\Delta cc$ together with $GABA_{B(2)}$, the EC_{50} values with 216 nM for SCH50911 and 2.4 nM for CGP54626 were near the dissociation constant values of these ligands for the wild-type receptor but the efficacy (maximal increase of FSK-stimulated cAMP accumulation) was about 4-fold lower (Fig. 5A). Protein levels of the various receptor subunits were similar in all three combinations as detected by Western blot (Fig. 5B) and [3H]CGP54626 binding. Because deletion of the coiled-coil region in $GABA_{B(2)}$ abolished this inverse agonist effect, we analyzed various combinations of $GABA_{B(1a)}$ and $GABA_{B(1a)}\Delta CT$ with $GABA_{B(2)}$ deletion mutants (Fig. 5D and Table 1). HEK293 cells cotransfected with $GABA_{B(1a)}$ and $GABA_{B(2)}$ deletions that lack the coiled-coil region (i.e., $GABA_{B(2)}\Delta cc$ and $GABA_{B(2)}\Delta CT$) did not show an increase in FSK-stimulated cAMP levels, whereas cotransfection with $GABA_{B(2)}\Delta 820–940$, $GABA_{B(2)}\Delta 748–780$, or $GABA_{B(2)}\Delta CT+cc$ showed an effect similar to that of the wild-type. If $GABA_{B(1a)}$ was replaced by $GABA_{B(1a)}\Delta CT$ in cotransfected HEK293 cells, the efficacy decreased to values similar to those with $GABA_{B(1)}\Delta cc$ + $GABA_{B(2)}$ (Fig. 5, A and D). In contrast to $GABA_{B(1a)}$, however, $GABA_{B(1a)}\Delta CT$ together with $GABA_{B(2)}\Delta 748–780$ or $GABA_{B(2)}\Delta CT+cc$ showed no significant inverse agonism (Fig. 5D and Table 1). In these two mutants, the coiled-coil region is located closer to the end of transmembrane domain 7 than in the wild-type $GABA_{B(2)}$ protein (see Fig. 1) which might affect receptor conformation. Thus, the C termini of both $GABA_{B(1)}$ and $GABA_{B(2)}$, and especially their ability to form a coiled coil, are important for allowing the receptor to adopt an activated conformation without an agonist bound.

Discussion

Physical Interaction And Trafficking of $GABA_B$ Receptor Subunits. Despite recent advances in our understanding of $GABA_B$ receptor heteromerization, the exact molecular determinants mediating the interaction between the two subunits are still unknown. Our data indicate that heteromerization and trafficking are strongly based on the coiled-coil interaction between the C termini of $GABA_{B(1)}$ and $GABA_{B(2)}$. At the same time, we found that deletion of the coiled-coil domains in $GABA_{B(1)}$ and $GABA_{B(2)}$ subunits did not completely abolish their physical interaction. Furthermore, $GABA_{B(2)}$ mutants lacking the coiled-coil domain led to significant surface expression of $GABA_{B(1)}$ and to a decreased, but significant amount of functional $GABA_B$ receptor heteromers (Fig. 3 and 4, $GABA_{B(1a)}$ + $GABA_{B(2)}\Delta cc$ and $GABA_{B(1a)}$ + $GABA_{B(2)}\Delta CT$). These data are in accordance with recent reports, which were published as this study was

in progress (Calver et al., 2001; Pagano et al., 2001) and suggest that besides the coiled-coil regions, additional interaction sites outside the C termini are responsible for the coassembly of the two $GABA_B$ receptor subunits. At least three observations speak in favor of an N-terminal interaction without excluding intramembranous interactions: $GABA_{B(1e)}$, a splice variant encoding an N-terminal fragment of $GABA_{B(1)}$, can compete with full-length $GABA_{B(1)}$ for binding to $GABA_{B(2)}$ (Schwarz et al., 2000); $GABA_{B(2)}$ contributes to high-affinity agonist binding (Jones et al., 1998; Kaupmann et al., 1998); and the extracellular domains of both $GABA_{B(1)}$ and $GABA_{B(2)}$ are involved in the mechanisms of receptor activation (Galvez et al., 2001). Indeed, other C family GPCRs form intermolecular disulfide bridges between their N-terminal extracellular domains and also show noncovalent interactions to support dimerization (Romano et al., 2001; Zhang et al., 2001).

Plasma membrane targeting of the $GABA_B$ receptor mainly depends on masking the short retention signal RSRR in the C terminus of $GABA_{B(1)}$ (Margeta-Mitrovic et al., 2000; Pagano et al., 2001; Fig. 2D). A chimeric $GABA_{B(2)}$ subunit in which the entire intracellular tail was replaced with the equivalent domain of $GABA_{B(1)}$ is retained intracellularly (Calver et al., 2001). However, our chimeric $GABA_{B(2)}$ subunit, $GABA_{B(2)}$_1CT922–960 (Fig. 1), very effectively reaches the cell surface. Thus, $GABA_{B(1)}$ deletion and chimeric constructs in this study revealed that whereas RSRR is certainly the main signal for retention of this subunit in the ER, it depends on the sequence environment to become recognized. A comparison of our results with those of Pagano et al. (2001) suggests that the amino acids directly N-terminal to RSRR, which at the same time form the C-terminal part of the coiled-coil domain (QLQXRQQLRSRR where X = S or D), are involved in its recognition (Fig. 6). The RSRR sequence is assumed to function by binding to an ER protein; it is tempting to speculate that this binding relies on a part of the $GABA_{B(1)}$ coiled-coil sequence as well. Competition between such an ER protein and $GABA_{B(2)}$ might then regulate the release of $GABA_{B(1)}$ from the ER. The $GABA_{B(1)}$ coiled-coil domain can have different binding partners depending on its subcellular localization within neurons; it has recently been

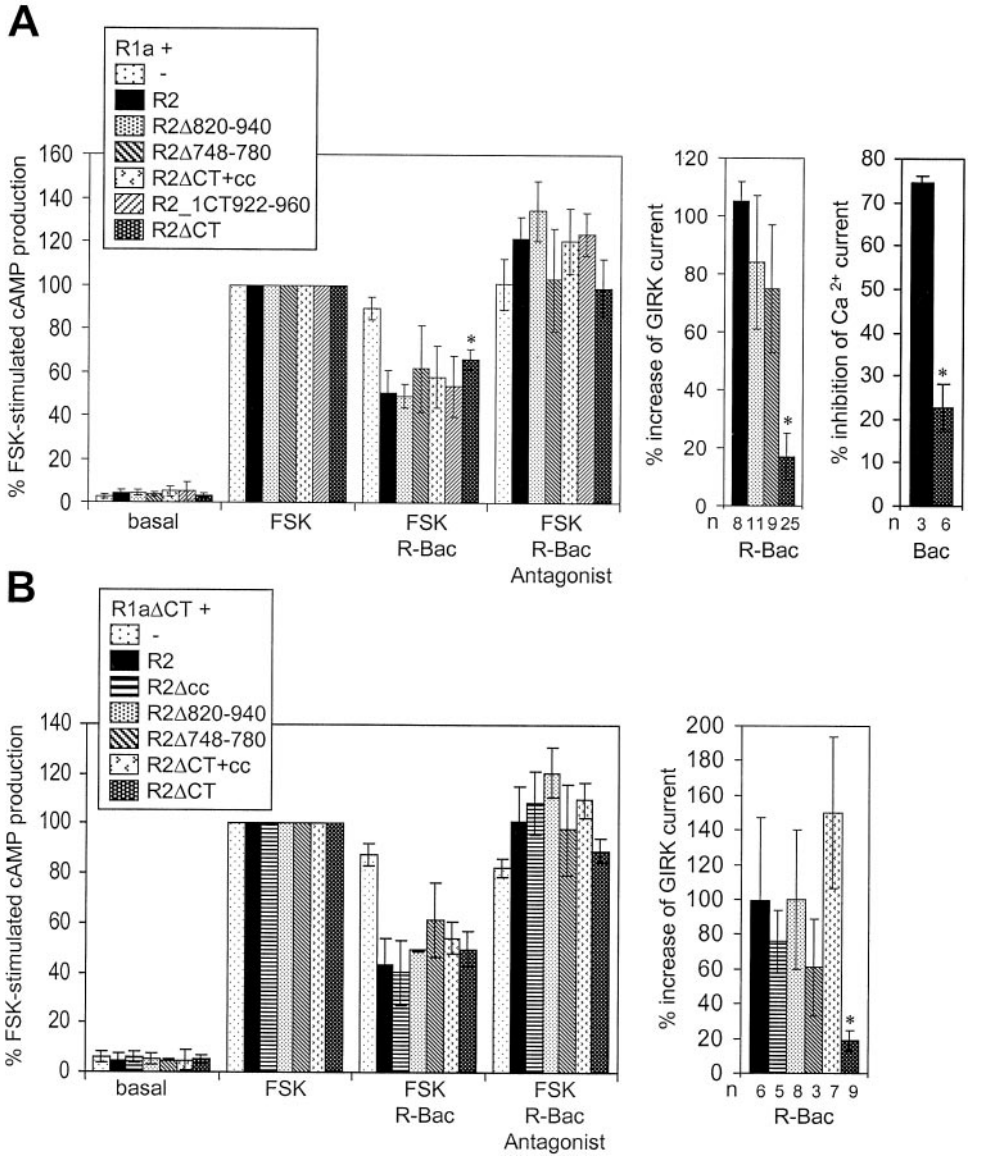

Fig. 4. Functional characterization of $GABA_B$ receptors consisting of $GABA_{B(1a)}$ (A) or $GABA_{B(1a)}\Delta CT$ (B) and $GABA_{B(2)}$ mutants. cAMP accumulation was measured in HEK293 cells cotransfected with the indicated constructs as outlined under *Materials and Methods*. cAMP production was stimulated using 2 μM FSK and inhibited with 100 μM *R*-baclofen (*R*-Bac). *R*-Bac was antagonized using either 2 mM SCH50911 or 10 μM CGP54626 (Antagonist). Results are presented as described in the legend of Fig. 3A and represent at least two independent experiments. Inhibition was significant ($p < 0.01$) for all cotransfected combinations as opposed to single $GABA_{B(1a)}$ or $GABA_{B(1a)}\Delta CT$ transfections. GIRK-activation and inhibition of Ca^{2+} channels was done as outlined in the legend to Fig. 3. Asterisks [*, $p <$ 0.01 (GIRKs) and *, $p < 0.05$ (cAMP level, Ca^{2+}-channels)] refer to reduced effector coupling compared with wild-type.

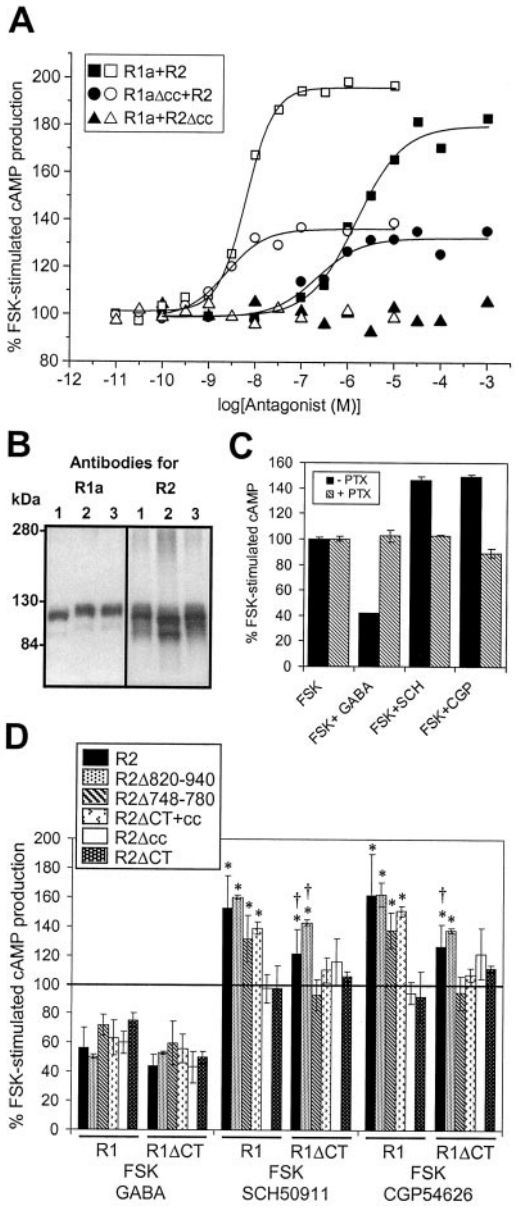

Fig. 5. Inverse agonism of $GABA_B$ receptor antagonists. A, HEK293 cells were cotransfected with the indicated constructs and FSK-stimulated cAMP production in the presence of increasing concentrations of the $GABA_B$ receptor antagonists SCH50911 (filled symbols) and CGP54626 (open symbols), respectively, was determined as outlined under *Materials and Methods*. cAMP production in the absence of ligand was set to 100% and is reported as a function of the antagonist concentration. Data points were fitted to the four-parameter logistic function using the program Origin (Microcal Software, Inc., Northampton, MA). The data shown are means of duplicates from one of three independent experiments. Expression levels and fitted parameters for this experiment are as follows: $GABA_{B(1a)}$ + $GABA_{B(2)}$: 900,000 [^{3}H]CGP54626 sites/cell, pEC_{50}(SCH50911) = 5.83 ± 0.09, pEC_{50}(CGP54626) = 8.21 ± 0.03; $GABA_{B(1a)}\Delta cc$ + $GABA_{B(2)}$: 730,000 [^{3}H]CGP54626 sites/cell, pEC_{50}(SCH50911) = 6.67 ± 0.22, pEC_{50} (CGP54626) = 8.63 ± 0.11; $GABA_{B(1a)}$ + $GABA_{B(2)}\Delta cc$: 920,000 [^{3}H]CGP54626 sites/cell. B, Western blot analysis of the cotransfected cells measured in A. Cell lysate of 100,000 cells was loaded in each lane: 1, $GABA_{B(1a)}\Delta cc$ + $GABA_{B(2)}$; 2, $GABA_{B(1a)}$ + $GABA_{B(2)}\Delta cc$; 3, $GABA_{B(1a)}$ + $GABA_{B(2)}$. The left three lanes were probed with a $GABA_{B(1)}$ -specific antiserum and the right three lanes with the $GABA_{B(2)}$ C terminus-specific antibody. C, the effect of 100 μM GABA, 1 mM SCH50911 (SCH) and 10 μM CGP54626 (CGP) on 2 μM FSK-stimulated cAMP levels was measured in HEK293 cells coexpressing $GABA_{B(1a)}$ and $GABA_{B(2)}$ with (▨) and without (■) prior treatment with 100 ng/ml pertussis toxin for 16 h. D, HEK293 cells were cotransfected with the expression plasmids for $GABA_{B(1a)}$ (R1) or $GABA_{B(1a)}\Delta CT$ (R1ΔCT) in combination with those for $GABA_{B(2)}$ (R2) and the indicated deletion mutants. cAMP production was measured in the presence of 2 μM FSK and either 100 μM GABA or 2 mM SCH50911 or 10 μM CGP54626, respectively. FSK-induced cAMP levels were set to 100% (horizontal line). Data in C and D are shown as percentage of FSK-induced cAMP levels under the indicated conditions and represent mean ± S.D. of at least two independent experiments. *, $p < 0.05$, antagonist effect on FSK-induced cAMP levels; †, $p < 0.05$, difference between $GABA_{B(1a)}$ and equivalent $GABA_{B(1a)}\Delta CT$ combinations.

found to even mediate binding of a transcription factor (Nehring et al., 2000; White et al., 2000).

Molecular Determinants for Coupling of $GABA_B$ Receptors with Effector Systems. Type C metabotropic receptors, such as the metabotropic glutamate receptors, couple to G-proteins via residues in their second and third intracellular loops (Gomeza et al., 1996). These residues are not conserved at parallel positions in $GABA_{B(1)}$, thereby raising the possibility that other loci within the intracellular loops or in the intracellular C termini of $GABA_B$ receptors mediate G-protein coupling. We therefore probed the ability of C-terminal mutants of $GABA_{B(1)}$ and of $GABA_{B(2)}$ to couple with each of their three main effector systems (i.e., adenylyl cyclase, GIRKs, and calcium channels).

An important caveat of functional experiments on receptor mutants done in vitro is their potential failure to effectively reach the cell surface (see $GABA_{B(1a)}$ + $GABA_{B(2)}\Delta cc$, $GABA_{B(1a)}$ + $GABA_{B(2)}\Delta CT$ and $GABA_{B(1a)}\Delta CT$ + $GABA_{B(2)}\Delta CT$). Comparison of effector coupling of $GABA_B$ receptor mutants versus their surface expression in our study clearly demonstrated that the C terminus of neither $GABA_{B(1)}$ nor of $GABA_{B(2)}$ is required for effector-coupling provided that the subunit combination reaches the cell surface effectively. These results, which are in perfect accordance with recent reports (Calver et al., 2001; Galvez et al., 2001; Pagano et al., 2001), suggest that the intracellular loops but not the C termini of $GABA_B$ subunits mediate G-protein coupling. Indeed, a study that was published during the preparation of this article identified by site-directed mutagenesis the amino acid residues located within the second intracellular loop of $GABA_{B(2)}$ that are critical for coupling of the $GABA_B$ heterodimer to downstream effector systems (Robbins et al., 2001). Taken together, these data suggest a model of $GABA_B$ heterodimers in which binding of agonists to $GABA_{B(1)}$ results in the activation of signaling cascades via G-protein coupling through $GABA_{B(2)}$.

Constitutive Activity of $GABA_B$ Receptors. Our data indicate that CGP54626 and SCH50911, which are well known as $GABA_B$ receptor antagonists, are also able to function as inverse agonists, because in $GABA_B$ receptor-expressing HEK293 cells, both ligands increase FSK-stimulated cAMP levels up to 2-fold. Being sensitive to treatment with pertussis toxin, this effect depends on a functional G-protein of the $G_{i/o}$ class. Our observations imply that CGP54626 and SCH50911 shift the $GABA_B$ receptor to a conformation that is less accessible to $G_{i\alpha}$, thus allowing higher activation of adenylyl cyclase. These results indicate that the $GABA_B$ receptor has the potential for constitutive activity. Galvez et al. (2001) observed a slight increase in the basal level of inositol phosphate formation in HEK293 cells expressing wild-type $GABA_B$ receptors. A large increase in the basal inositol phosphate formation was detectable in cells expressing $GABA_B$ receptor dimers consisting of $GABA_{B(1a)}$ and a chimeric $GABA_{B(2)}$ subunit, in which the extracellular do-

main has been replaced by that of $GABA_{B(1a)}$. This large increase in inositol phosphate could be partly inhibited by GABA and this inhibition could be antagonized by CGP64213.

Constitutive activity has been described for numerous GPCRs (Leurs et al., 1998). In most cases, inverse agonism and constitutive activity have been observed in heterologous systems, in which receptors are often expressed at very high densities. In the last few years, constitutive activity has also been shown for some recombinant receptors expressed at physiological concentrations (Smit et al., 1996; Claeysen et al., 1999). Thus, it would be of great interest to determine whether constitutive activity of $GABA_B$ receptors exists at physiological levels in stable cell lines or in native tissue. Evidence for the relevance of constitutive activity of GPCRs in vivo is emerging and might enable therapeutic applications for inverse agonists (Morisset et al., 2000).

Interestingly, deletion of the coiled-coil region within the C terminus of $GABA_{B(2)}$ abolished the ability of the two antagonists CGP54626 and SCH50911 to increase FSK-stimulated cAMP levels whereas deletion of the regions upstream or downstream of the coiled-coil stretch had no significant effect on inverse agonism. Deletion of the coiled-coil region within the C terminus of $GABA_{B(1a)}$ decreased the efficacy of CGP54626 and SCH50911 to function as inverse agonists but did not abolish inverse agonism. Our data on coupling to adenylyl cyclase can be interpreted in the framework of the simple, two-state model of GPCR activation, where the receptor can isomerize from an inactive conformation (R), which is not able to activate G-proteins, to an active form (R*) in the absence of an agonist (Lefkowitz et al., 1993). Our data indicate that the active conformation is stabilized by the coiled-coil interaction. If the coiled-coil cannot be formed because of its deletion in $GABA_{B(2)}$, then the $GABA_B$ heteromer cannot adopt an active conformation without an agonist bound. Deletion of the coiled coil in $GABA_{B(1)}$ or of its whole cytoplasmic C-terminal part still allows constitutive activity as long as the coiled-coil region in $GABA_{B(2)}$ is neither deleted nor displaced. However, the equilibrium is shifted toward the inactive form, thus reducing the efficacy. Thus, as opposed to agonist-mediated G-protein coupling, both C termini are involved in efficiently mediating the inverse agonist effect of the ligands CGP54626 and SCH50911. In different GPCR families, different receptor domains are of importance for constraining the receptor in inactive and active conformations. There are increasing data to indicate that specific sequences of the C-terminal end of GPCRs, including

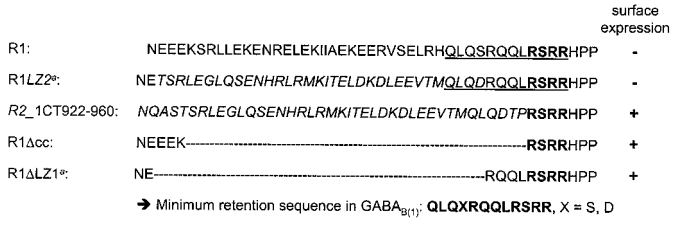

Fig. 6. The functionality of the retention signal RSRR depends on surrounding sequences. The sequences of the coiled-coil region of wild-type $GABA_{B(1)}$ and mutants are shown. In the chimeric constructs, sequences derived from $GABA_{B(2)}$ are italic. The retention signal reported in Margeta-Mitrovic et al. (2000) is bold. The functional retention sequence deduced from a combination of results described in this study and in constructs characterized by Pagano et al. (2001) is underlined. +, surface expression.

metabotropic glutamate receptor 1 (Mary et al., 1998), histamine (Morisset et al., 2000), or serotonin receptors (Claeysen et al., 1999), modulate the isomerization of these receptors from R to R*. In contrast to the $GABA_B$ receptor, however, the role of the C termini of the above receptors is to maintain the receptor in an inactive conformation in the absence of an agonist.

Conclusions. Interaction of the two subunits of the $GABA_B$ receptor occurs not only through the coiled-coil domains but also through low affinity interaction sites, probably located within N-terminal extracellular domains and/or membrane spanning regions. Whereas the C termini of the two subunits are not necessary for functional heterodimerization, their coiled-coil domains are involved in stabilizing the active conformation of the heterodimer. Furthermore, efficient trafficking of $GABA_{B(1)}$ to the cell surface requires interaction via the coiled-coil domain. Notably, the retention signal of $GABA_{B(1)}$ requires a part of its coiled-coil sequence.

Acknowledgments

We thank G. Eichberger, G. Eisenhardt, F. Herzog, A. Hesselschwerdt, and K. Hirschfeld for excellent technical assistance.

References

Bai M, Trivedi S, Kifor O, Quinn SJ, and Brown EM (1999) Intermolecular interactions between dimeric calcium-sensing receptor monomers are important for its normal function. *Proc Natl Acad Sci USA* **96:**2834–2839.

Bowery NG (1993) $GABA_B$ receptor pharmacology. *Annu Rev Pharmacol Toxicol* **33:**109–147.

Calver AR, Robbins MJ, Cosio C, Rice SQ, Babbs AJ, Hirst WD, Boyfield I, Wood MD, Russell RB, Price GW, et al. (2001) The C-terminal domains of the $GABA_b$ receptor subunits mediate intracellular trafficking but are not required for receptor signaling. *J Neurosci* **21:**1203–1210.

Claeysen S, Sebben M, Becamel C, Bockaert J, and Dumuis A (1999) Novel brain-specific 5-HT_4 receptor splice variants show marked constitutive activity: role of the C-terminal intracellular domain. *Mol Pharmacol* **55:**910–920.

Couve A, Filippov AK, Connolly CN, Bettler B, Brown DA, and Moss SJ (1998) Intracellular retention of recombinant GABAB receptors. *J Biol Chem* **273:**26361–26367.

Couve A, Moss SJ, and, Pangalos MN (2000) $GABA_B$ receptors A new paradigm in G protein signaling. *Mol Cell Neurosci* **16:**296–312.

Filippov AK, Couve A, Pangalos MN, Walsh FS, Brown DA, and Moss SJ (2000) Heteromeric assembly of $GABA_BR1$ and $GABA_BR2$ receptor subunits inhibits Ca^{2+} current in sympathetic neurons. *J Neurosci* **20:**2867–2874.

Galvez T, Duthey B, Kniazeff J, Blahos J, Rovelli G, Bettler B, Prezeau L, and Pin JP (2001) Allosteric interactions between GB1 and GB2 subunits are required for optimal $GABA_B$ receptor function. *EMBO (Eur Mol Biol Organ) J* **20:**2152–2159.

Gomeza J, Joly C, Kuhn R, Knöpfel T, Bockaert J, and Pin JP (1996) The second intracellular loop of metabotropic glutamate receptor 1 cooperates with the other intracellular domains to control coupling to G-proteins. *J Biol Chem* **271:**2199–2205.

Ikeda SR (1996) Voltage-dependent modulation of N-type calcium channels by G-protein beta gamma subunits. *Nature (Lond)* **380:**255–258.

Ikeda SR (1997) Heterologous expression of receptors and signaling proteins in adult mammalian sympathetic neurons by microinjection. *Methods Mol Biol* **83:**191–202.

Jones KA, Borowsky B, Tamm JA, Craig DA, Durkin MM, Dai M, Yao WJ, Johnson M, Gunwaldsen C, Huang LY, et al. (1998) $GABA_B$ receptors function as a heteromeric assembly of the subunits $GABA_BR1$ and $GABA_BR2$. *Nature (Lond)* **396:**674–679.

Jordan BA and Devi LA (1999) G-protein-coupled receptor heterodimerization modulates receptor function. *Nature (Lond)* **399:**697–700.

Kammerer RA, Frank S, Schulthess T, Landwehr R, Lustig A, and Engel J (1999) Heterodimerization of a functional GABAB receptor is mediated by parallel coiled-coil alpha-helices. *Biochemistry* **38:**13263–13269.

Kaupmann K, Huggel K, Heid J, Flor PJ, Bischoff S, Mickel SJ, McMaster G, Angst C, Bittiger H, Froestl W, et al. (1997) Expression cloning of $GABA_B$ receptors uncovers similarity to metabotropic glutamate receptors. *Nature (Lond)* **386:**239–246.

Kaupmann K, Malitschek B, Schuler V, Heid J, Froestl W, Beck P, Mosbacher J, Bischoff S, Kulik A, Shigemoto R, et al. (1998) $GABA_B$-receptor subtypes assemble into functional heteromeric complexes. *Nature (Lond)* **396:**683–687.

Kuner R, Köhr G, Grünewald S, Eisenhardt G, Bach A, and Kornau HC (1999) Role of heteromer formation in GABAB receptor function. *Science (Wash DC)* **283:**74–77.

Lefkowitz RJ, Cotecchia S, Samama P, and Costa T (1993) Constitutive activity of receptors coupled to guanine nucleotide regulatory proteins. *Trends Pharmacol Sci* **4:**03–307.

Leurs R, Smit MJ, Alewijnse AE, and Timmerman H (1998) Agonist-independent

regulation of constitutively active G-protein-coupled receptors. *Trends Biochem Sci* **3:**18–422.
Margeta-Mitrovic M, Jan YN, and Jan LY (2000) A trafficking checkpoint controls $GABA_B$ receptor heterodimerization. *Neuron* **27:**97–106.
Mary S, Gomeza J, Prezeau L, Bockaert J, and Pin JP (1998) A cluster of basic residues in the carboxyl-terminal tail of the short metabotropic glutamate receptor 1 variants impairs their coupling to phospholipase C. *J Biol Chem* **273:**425–432.
Morisset S, Rouleau A, Ligneau X, Gbahou F, Tardivel-Lacombe J, Stark H, Schunack W, Ganellin CR, Schwartz JC, and Arrang JM (2000) High constitutive activity of native H3 receptors regulates histamine neurons in brain. *Nature (Lond)* **408:**860–864.
Nehring RB, Horikawa HP, El Far O, Kneussel M, Brandstätter JH, Stamm S, Wischmeyer E, Betz H, and Karschin A (2000) The metabotropic GABAB receptor directly interacts with the activating transcription factor 4. *J Biol Chem* **275:** 35185–35191.
Ng GY, Clark J, Coulombe N, Ethier N, Hebert TE, Sullivan R, Kargman S, Chateauneuf A, Tsukamoto N, McDonald T, et al. (1999) Identification of a GABAB receptor subunit, gb2, required for functional GABAB receptor activity. *J Biol Chem* **274:**7607–7610.
Pagano A, Rovelli G, Mosbacher J, Lohmann T, Duthey B, Stauffer D, Ristig D, Schuler V, Meigel I, Lampert C, et al. (2001) C-terminal interaction is essential for surface trafficking but not for heteromeric assembly of $GABA_b$ receptors. *J Neurosci* **21:**1189–1202.
Prosser HM, Gill CH, Hirst WD, Grau E, Robbins M, Calver A, Soffin EM, Farmer CE, Lanneau C, Gray J, et al. (2001) Epileptogenesis and enhanced prepulse inhibition in $GABA_{B1}$-deficient mice. *Mol Cell Neurosci* **7:**059–1070.
Robbins MJ, Calver AR, Filippov AK, Hirst WD, Russell RB, Wood MD, Nasir S, Couve A, Brown DA, Moss SJ, et al. (2001) $GABA_{B2}$ is essential for G-protein coupling of the $GABA_B$ receptor heterodimer. *J Neurosci* **21:**8043–8052.
Rocheville M, Lange DC, Kumar U, Patel SC, Patel RC, and Patel YC (2000a) Receptors for dopamine and somatostatin: formation of hetero-oligomers with enhanced functional activity. *Science (Wash DC)* **288:**154–157.
Rocheville M, Lange DC, Kumar U, Sasi R, Patel RC, and Patel YC (2000b) Subtypes of the somatostatin receptor assemble as functional homo- and heterodimers. *J Biol Chem* **275:**7862–7869.
Romano C, Miller JK, Hyrc K, Dikranian S, Mennerick S, Takeuchi Y, Goldberg MP, and O'Malley KL (2001) Covalent and noncovalent interactions mediate metabotropic glutamate receptor $mGlu_5$ dimerization. *Mol Pharmacol* **59:**46–53.
Romano C, Yang WL, and O'Malley KL (1996) Metabotropic glutamate receptor 5 is a disulfide-linked dimer. *J Biol Chem* **271:**28612–28616.
Salahpour A, Angers S, and Bouvier M (2000) Functional significance of oligomerization of G-protein-coupled receptors. *Trends Endocrinol Metab* **1:**63–168.
Schall TJ, Lewis M, Koller KJ, Lee A, Rice GC, Wong GH, Gatanaga T, Granger GA, Lentz R, and Raab H (1990) Molecular cloning and expression of a receptor for human tumor necrosis factor. *Cell* **61:**361–370.
Schuler V, Luscher C, Blanchet C, Klix N, Sansig G, Klebs K, Schmutz M, Heid J, Gentry C, Urban L, et al. (2001) Epilepsy, hyperalgesia, impaired memory, and loss of pre- and postsynaptic $GABA_B$ responses in mice lacking $GABA_{B(1)}$. *Neuron* **31:**47–58.
Schwarz DA, Barry G, Eliasof SD, Petroski RE, Conlon PJ, and Maki RA (2000) Characterization of gamma -aminobutyric acid receptor $GABAB_{1e}$, a $GABAB_1$ splice variant encoding a truncated receptor. *J Biol Chem* **275:**32174–32181.
Smit MJ, Leurs R, Alewijnse AE, Blauw J, Van Nieuw Amerongen GP, Van De Vrede Y, Roovers E, and Timmerman H (1996) Inverse agonism of histamine H2 antagonist accounts for upregulation of spontaneously active histamine H2 receptors. *Proc Natl Acad Sci USA* **93:**6802–6807.
White JH, McIllhinney RA, Wise A, Ciruela F, Chan WY, Emson PC, Billinton A, and Marshall FH (2000) The GABAB receptor interacts directly with the related transcription factors CREB2 and ATFx. *Proc Natl Acad Sci USA* **97:**13967–13972.
White JH, Wise A, Main MJ, Green A, Fraser NJ, Disney GH, Barnes AA, Emson P, Foord SM, and Marshall FH (1998) Heterodimerization is required for the formation of a functional $GABA_B$ receptor. *Nature (Lond)* **396:**679–682.
Zhang Z, Sun S, Quinn SJ, Brown EM, and Bai M (2001) The extracellular calcium-sensing receptor dimerizes through multiple types of intermolecular interactions. *J Biol Chem* **276:**5316–5322.

Address correspondence to: Dr. Sylvia Grünewald, Axaron Bioscience AG, Im Neuenheimer Feld 515, D-69120 Heidelberg, Germany. E-mail: gruenewald@axaron.com